

Appendix D

Characterization of Bubble Column Slurry Phase Iron Fischer-Tropsch Catalysts

Yaming Jin and Abhaya K. Datye

Center for Microengineered Materials and Department of Chemical & Nuclear Engineering,
University of New Mexico, Albuquerque, NM 87131, USA

Abstract

The cross-sectional transmission electron microscopy (XTEM) method and x-ray diffraction (XRD) were used for phase analysis of bubble column slurry phase iron Fischer-Tropsch catalysts. For the deactivated LGX-171, the carbide phase shows mono-dispersion characteristic. The carbide particles have well-defined shape, spherical or rectangular, and give a distinctive c-carbide XRD pattern. The average particle size, 39.4 nm, by XRD was in good agreement with statistical value of 37.5 nm by TEM. On the other hand, two carbide phases are found to coexist in the active catalyst: big twisted particles (20-40 nm) and highly dispersed carbide particles (less than 10 nm). High resolution TEM work shows that the big distorted carbide particles belong to e'-carbide, while the highly dispersed carbide phase is most probably a mixture of e'-carbide and c-carbide. For this particular set of iron catalysts, big faceted magnetite single crystals were found to be present in the catalyst both at the active and deactivated states. From these, we conclude that the e'-carbide must represent the active phase in Fe F-T catalysts.

1. Introduction

Fischer-Tropsch Synthesis is recognized as a viable route for conversion of syngas to liquid fuels (1). This study is directed at understanding mechanisms of catalyst deactivation in Fe catalysts used in a slurry phase reactor. We report here analyses of end-of-run catalysts from two F-T runs. The catalyst reactivity has been reported elsewhere (2), but in the previous work, we were unable to conclusively identify the causes of catalyst deactivation.

It is recognized that loss of surface area of the catalytically active phase and deposition of unreactive carbonaceous deposits must constitute possible mechanisms for catalyst deactivation (2,3). However, there is as yet no consensus on the nature of the active phase in Fe F-T catalysts. Previous work has tried to correlate bulk phase information with catalytic reactivity based on results of analytical methods such as Mössbauer spectroscopy (MS) and X-ray diffraction (XRD) techniques. Besides the intrinsic limitations of these bulk techniques for the quantification of a highly dispersed iron phase (with particles less than 10 nm), there are several other experimental difficulties in determining an accurate phase composition of slurry bubble column F-T catalysts. The catalyst removed from the reactor is dispersed in product wax at a loading of 5 wt%, hence a wax removal step is usually performed prior to analysis. We have recently (4) shown that Soxhlet extraction, the commonly used wax removal procedure, can cause oxidation of the

reduced iron phases. Furthermore, the wax is often crystalline and interferes with the diffraction peaks from the iron carbide phases of interest. We have also found that there are enormous differences in scattering factors for the various iron phases making quantitative analysis based on peak heights completely unreliable (4). We believe that some of these experimental difficulties have resulted in the generally accepted conclusion that there is no clear relationship between catalyst activity and the phase composition of the working catalyst.

In order to get accurate phase information of working FTS catalysts, and to minimize problems with surface oxidation of the reduced iron phases, we feel it is necessary to characterize working iron catalysts protected by the hydrocarbon wax (4). Quantitative Rietveld structure refinement analysis allowed us to obtain useful phase information of the wax-containing iron catalyst sample. Nevertheless, the peak overlaps between the crystalline wax and iron phases of interest, and the low diffraction peak intensities suggested that the XRD analysis be corroborated with other methods. In this paper, we report a cross-section transmission electron microscope (XTEM) study of the phases present in working Fe FTS catalysts. The TEM results along with XRD analysis helps to provide a more comprehensive picture of these catalysts.

2. Experimental

The catalyst sample studied in this paper has a chemical composition of 100Fe/4.4Si/1.0K and was provided to us by Dr. Burtron Davis at the Center of Applied Energy Research (CAER), University of Kentucky, after use in FT synthesis runs. In run LGX-171, the precipitated oxide precursor was pretreated with syngas at 1 atm and 270°C for 24 hours, then underwent FTS at 270°C, 175 psig. The wax-mixed catalyst sample was removed from the slurry reactor after time-on-stream (TOS) 3164 hours. The catalyst activity was high for the first 2800 hours of this run, but over the last few hundred hours there was a rapid deactivation and the catalyst was removed at the end of run where CO conversion was 20%. On the other hand, in run LGX-175, the catalyst precursor was pretreated in CO at 1 atm and 270°C for 24 hours and underwent FTS at the same conditions as LGX-171. The catalyst sample was removed after TOS 1160 hours while its CO conversion was 79%. Detailed reactivity data were reported elsewhere (2,5).

XRD data were obtained on a Scintag PAD-V powder diffractometer using Cu-K α radiation ($\lambda=1.5406 \text{ \AA}$). Scans were taken from 10° to 90° in step-scan mode, 0.04° per step, 0.4° per minute. For cross section TEM, the wax-mixed iron catalysts were first embedded in Spürr's low viscosity epoxy. After curing the epoxy, sections with thickness about 40-60 nm were prepared. The microtomed sample sections were mounted on TEM grids with holey carbon film and examined in a JEOL 2010 HRTEM microscope operated at 200 KeV. These thin sections allow us to get high resolution images that permit detailed phase identification, and also to get particle size distributions for each iron phase.

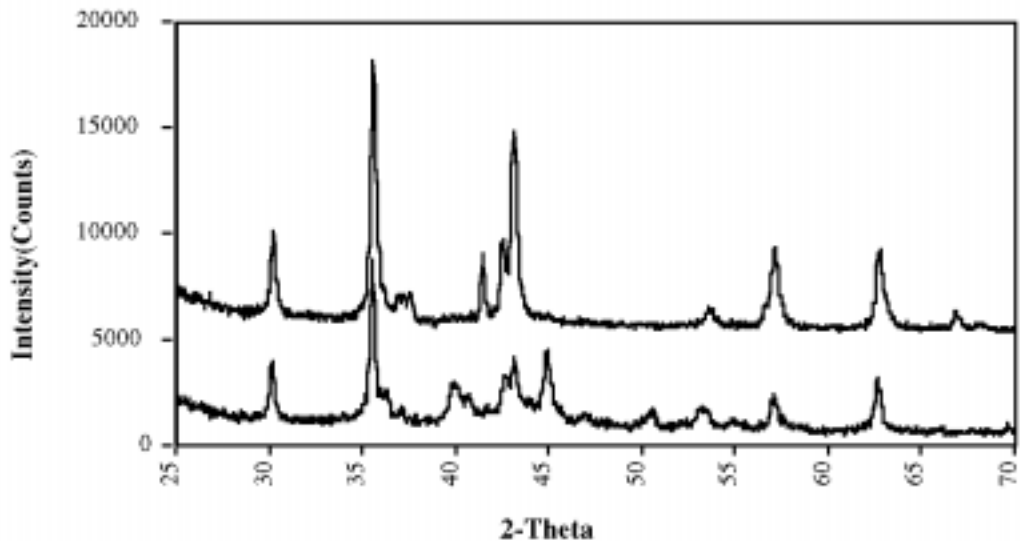


Figure 1 XRD spectra of LGX-171 (upper) deactivated catalyst and LGX-175 (lower), active catalyst after partial removal of hydrocarbon wax.

3. Results

The XRD spectra of LGX-171 and LGX-175 with wax partly removed are shown in figure 1. Two phases, magnetite and c-carbide, can be clearly identified in the XRD spectrum of LGX-171 (the low activity catalyst). The average particle size estimated by Scherrer's equation is 27.2 nm and 39.4 nm for the two phases respectively. The catalyst from run LGX-175 (high activity) also

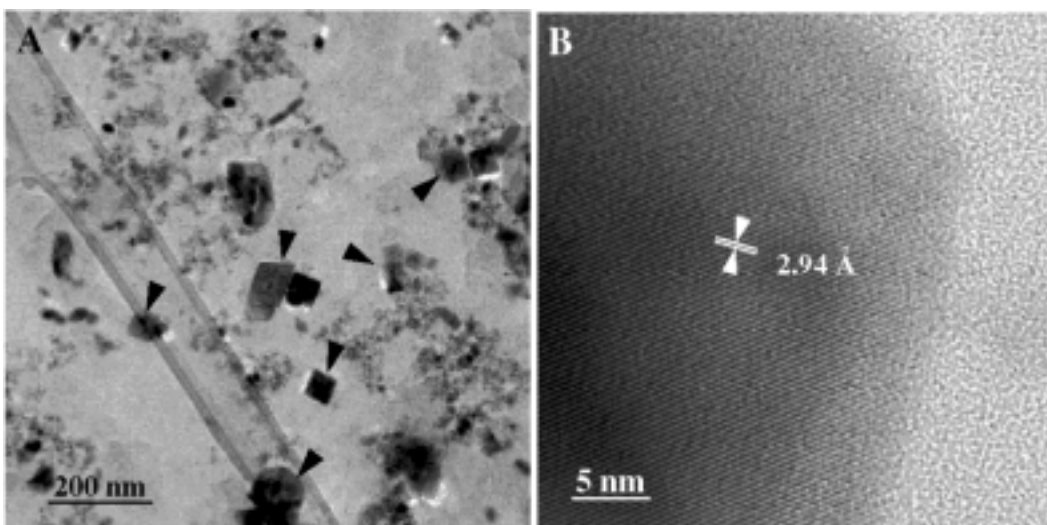


Figure 2 XTEM images of LGX-175. **A)** Low mag overview, the large magnetite single crystals are highlighted; **B)** High mag image of one of these faceted particles.

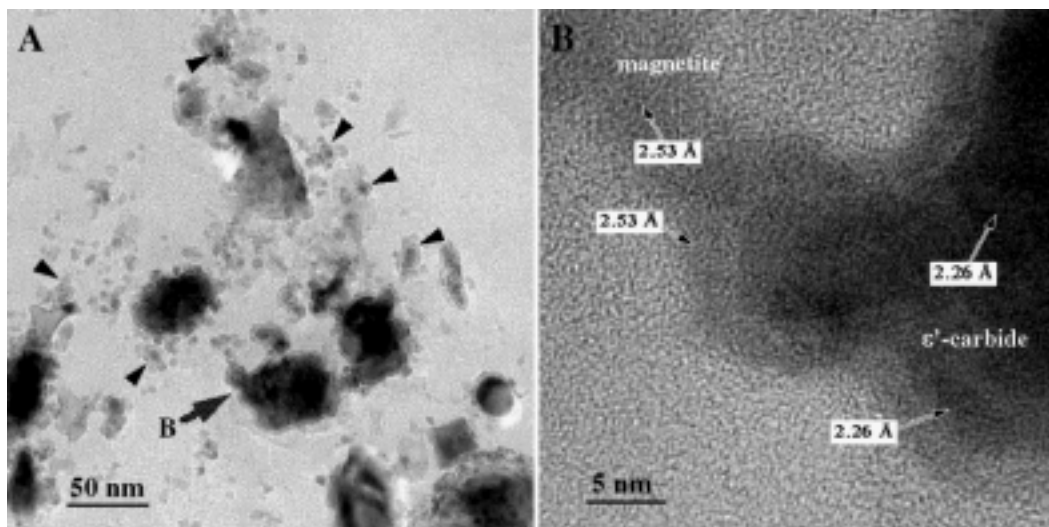


Figure 3 Fig. 3 TEM images showing the complex microstructure of sample LGX-175. **A)** Low mag view of 3 distinct phases: large distorted e'-carbide particles, fine carbide particles (some are highlighted), and highly dispersed magnetite particles. **B)** High mag view showing the coexistence of these 3 phases.

shows pronounced magnetite peaks with an estimated average particle diameter of 30.3 nm. However, the nature of the carbide peaks is very different from those in LGX-171. From the intensity of the (002) diffraction peak of c'-carbide at $2\theta=41.45^\circ$ which does not interfere with the other peaks, we can see that very little c'-carbide is present in LGX-175. On the other hand, the broad diffraction peaks at $2\theta=44.96^\circ$ and 40.00° match the (121) and (120) diffraction lines of e'-carbide. By using Scherrer's equation, we can estimate the average particle size of e'-carbide to be 19.2 nm.

Figure 2 shows XTEM images of the sample from LGX-175 (figure 2-A). Large (around 50 nm) faceted particles are seen to be sparsely dispersed in this image. By analyzing the high resolution images, we can conclusively identify these particles as magnetite single crystals, as shown in figure 2- B (2.94 Å corresponds to the (220) plane of magnetite). The rest of the catalyst is a complex mixture of iron phases. A typical view is shown in figure 3-A. Closer examination shows three different types of iron phases to be present in this particular sample. There are big distorted particles (20 to 40 nm) always with a surface layer or smaller particles sticking to them (figure 3-A). High resolution images of these iron phases have lattice spacings of 2.26 Å and 2.02 Å correspond to d-values of (120) and (121) planes of e'-carbide. Therefore, we attribute this phase to be e'-carbide. The rest of the catalyst contains highly dispersed particles (usually less than 10 nm) as shown in figure 3-A. Those without a surface layer are identified as fine magnetite particles, shown in figure 3-B (the 2.53 Å spacing corresponds to the d-value of the (311) plane of magnetite). The fact that magnetite lattice fringes are also seen on the surface of the carbide suggests that the highly dispersed magnetite may actually be a passivating oxide formed due to air exposure. The particles with a surface layer marked in figure 3-A are identified

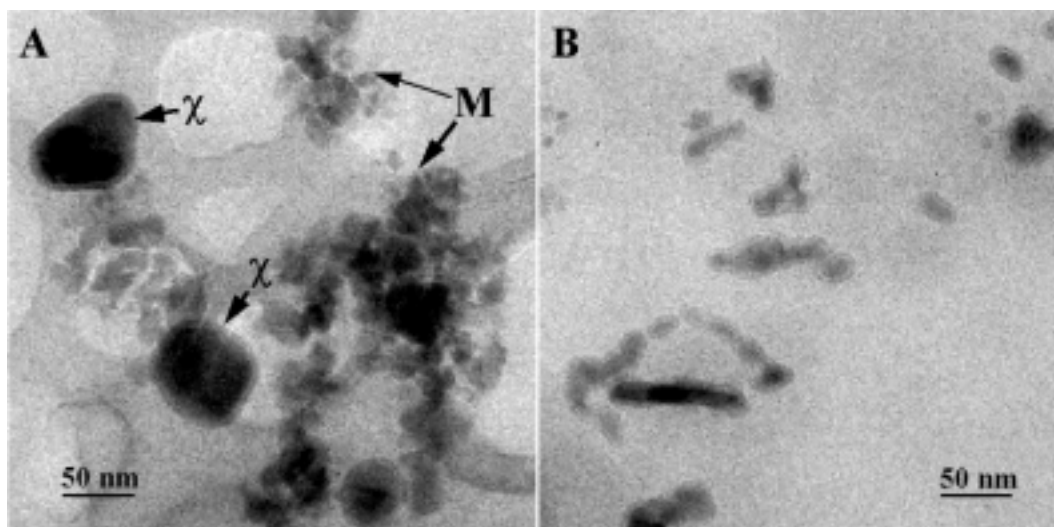


Figure 4 Comparison of carbide phases in LGX-171 (deactivated) and LGX-175 (active). A) Regular shaped c-carbide particles in LGX-171 B) Highly dispersed carbide particles seen in LGX-175 (active catalyst) are missing in sample LGX-171.

as highly dispersed iron carbide. High resolution imaging has revealed that these particles exhibit lattice fringes of e'-carbide as well as c-carbide. These carbide particles do not necessarily coexist with the fine magnetite particles as seen in figure 3-A. In fact this phase was found to be well dispersed everywhere in the sample.

In contrast to sample LGX-175 (the active catalyst), sample LGX-171 (the deactivated catalyst) only showed the presence of c-carbide in addition to the magnetite, both by XRD and TEM. These c-carbide particles had smooth surfaces, and well defined shapes - rectangular or spherical. All of these particles have a uniform surface layer having a thickness of about 3-4 nm (fig. 4-A). The average particle diameter, 39.4 nm by XRD, is consistent with the estimated average diameter of 37.5 nm by TEM. There are also large magnetite single crystals dispersed in this sample similar to those seen in LGX-175. In addition, there is a polycrystalline magnetite phase distributed throughout this catalyst sample. However, unlike the LGX-175 (active) sample, the size of these magnetite particles is larger (about 10 to 20 nm), and those particle always form agglomerates as shown in Figure 4-A.

4. Discussion

In this work, we have analyzed two used FT synthesis catalyst samples by XRD and TEM. The XRD shows e'-carbide to be present in LGX-175 but only c-carbide to be present in LGX-171. It also appears that the e'-carbide peak seen in XRD comes mainly from the distorted, large e'-carbide particles seen in LGX-175 and the highly dispersed carbide particles appear to be missed completely by XRD. However, much of the surface area must come from the highly dispersed carbide phase that is seen in the active catalyst but totally absent from the deactivated catalyst.

Hence, analysis of the active phase must consider this highly dispersed phase. Considering the particle size of this carbide phase, we feel that this phase has most probably been missed by bulk analytical methods such as XRD and Mössbauer (particularly at room temperature where it would be superparamagnetic). This highly dispersed phase is actually a mixture of e'-carbide and c-carbide (as determined from lattice fringe spacings) and it is difficult to quantify the ratio of these two kinds of carbide by TEM alone (which only looks at a small region of the sample). It would be necessary to perform Mössbauer spectroscopy of these samples at liquid He temperatures and correlate with the TEM images to get at the true distribution of these phases. Without this data, we can state that the high activity of catalyst LGX-175 must be related, at least in part, to the presence of the highly dispersed carbide phase. Furthermore, since e'-carbide is the major bulk carbide phase seen in the active catalyst (by XRD), and it is completely absent in the deactivated catalyst, we feel comfortable in stating that the bulk e'-carbide must be more active than the bulk c-carbide.

In the above analysis, we have ignored the presence of the magnetite: the large single crystals as well as the highly dispersed magnetite. With H₂O and CO₂ being by-products of F-T synthesis (their ratio being determined by the extent of water gas shift), we can expect some magnetite to be present as a result of oxidation caused by these molecules. However, in a previous study (4) where the hot wax had been carefully removed under an inert blanket, we found neither the large magnetite crystals nor the dispersed phase. Other recent work (6) involving samples that were not exposed to air before analysis also confirms the absence of magnetite in the catalyst used for F-T synthesis. Hence, we suggest that the magnetite seen here may have two different origins. Since these two samples were both removed from the reactor without an inert protective environment while the slurry was still hot, we think part of the fine magnetite phase could arise due to oxidation of the iron carbide during slurry removal. In the case of LGX-175, we have also seen a magnetite layer on the surface of the iron carbide., analogous to a passivating layer of oxide seen in our previous work on air exposed samples (7). The large faceted magnetite single crystals are present in both the active catalyst (LGX-175) and inactive catalyst (LGX-171). They could not arise from an oxidation of the iron phase during slurry removal. We conclude that these magnetite particles represent unreduced magnetite from the catalyst precursor. Our previous work (8) has shown that magnetite that had a Swiss-cheese (porous) morphology could be readily reduced to iron carbide. The more perfect, faceted magnetite particles must be harder to reduce and hence they persist even after 3000 hours of reaction in syngas, a possibility we will investigate in our future work.

To summarize, we can conclude that the active F-T catalysts consists of a mixture of highly dispersed carbide phase and bulk e'-carbide. In the deactivated catalyst, both e'-carbide and the dispersed carbide were missing. This leaves open the question of how and why the catalyst in run LGX-171 deactivated, since it appeared to run at high conversion for over 2800 hours. Since, no samples are available of the catalyst in its active state, we can only speculate that a process upset may have caused transformation of the active dispersed carbide phase into a mixture of magnetite and c-carbide. It is clear that in its deactivated form the catalyst contains plenty of c-carbide, but show very low activity. Therefore, it appears that the e'-carbide must

represent the active phase in Fe F-T catalysts. Future work will attempt to correlate these observations with Mössbauer spectroscopy which should permit quantification of the phase composition of these working F-T catalysts. We conclude that XTEM provides valuable insight for understanding the microstructure of Fe catalysts used for F-T synthesis.

Financial support for this work from the US Department of Energy, FETC university coal research grant DE-FG-22-95PC95210 is gratefully acknowledged. We thank Dr. Burtron Davis for providing the catalyst samples whose analysis is reported here.

References

1. Xu, L., Bao, S., O'Brien, R.J., Raje, A. and Davis, B.H., *ChemTech* 47, 1998.
2. Jackson, N.B., Datye, A.K., Mansker, L.D., O'Brien, R.J. and Davis, B.H., in *Catalyst Deactivation*, (Bartholomew, C.H. and Fuentes, G.A. eds.), *Stud. Surf. Catal.*, 111, 501 (1997).
3. Eliason, S.A. and Bartholomew, C.H., *ibid*, 517 (1997).
4. Mansker, L. D., Jin, Y., Bukur, D. B. and Datye, A. K., submitted to *Appl. Catal.*, 1998.
5. O'Brien, R.J., Xu, L., Spicer, R.L. and Davis, B.H., *Energy and Fuels*, 10(4), 921 (1996).
6. Mahajan, D., et al., *Energy and Fuels*, in press
7. Shroff, M.D. and Datye, A.K., *Catal. Lett.*, 37, 101 (1996)
8. Shroff, M.D., Kalakkad, D.S., Coulter, K.E., Kohler, S.D., Harrington, M.S., Jackson, N.B., Sault, A.G., and Datye, A.K., *J. Catal.*, 156(2), 185 (1995).